Stiffness Metrics for Design of 3-RRR Flexible Manipulator

K.V.Varalakshmi[1], Dr.J.Srinivas[2]
Department of Mechanical Engineering, NIT Rourkela-769 008, India

Abstract : This paper presents the kinematics and stiffness analysis of flexible parallel manipulators. As a primary step, the forward kinematic solutions are obtained using soft computing approaches based on Genetic Algorithms (GAs) and Neural networks (NN) and workspace configuration is arrived. The Jacobian and platform stiffness matrices are evaluated within the defined workspace. The flexible link configuration with compliant joints is analyzed using a pseudo rigid-body model. The revolute joint compliance is considered with narrow rectangular flexure hinges which are idealized as equivalent torsional springs in pseudo rigid-body model. Having the defined link dimensions and joint cross-sections at any configuration, the model is discritized with frame and plate elements and the assembled system is analyzed statically and dynamically. The methodology is illustrated with 3-RRR flexible parallel manipulator and the results are compared with commercial software solution.

Keywords: Kinematics, Workspace, Flexible links, Forward kinematics, Pseudo rigid body model.

I.   Introduction

Nowadays parallel manipulators have become an attractive topic of interest in several applications, such as machine tools, motion simulators, micro robots, medical devices and physical sensors, due to their intrinsic advantages in the factors of payload, stiffness, accuracy, operational velocity and acceleration. Parallel manipulators which are closed kinematic structures composed of two platforms interconnected by few links. The top platform (referred to as end-effector) is the mobile one controlled with respect to the base platform through variable link lengths to obtain the final position and orientation of the end-effector. The inverse kinematics of such manipulators, which maps the task space to the joint space, is a straight-forward problem; while the direct kinematics is often complex involving multiple solutions in Cartesian space. Direct kinematics is concerned with the determination of the end-effector pose from the given set of link lengths or joint angles. It has no closed form solution since it involves solving a series of simultaneous nonlinear algebraic equations and non-unique multiple set of solutions referred to the assembly modes, are obtained from one set of data.

Several approaches have been proposed for the forward kinematics of such manipulators. The analytical approach formulates a system of nonlinear equations and then converts it to a high degree univariate polynomial which can be solved by numerical techniques. It has been shown that for the most general parallel manipulators, this approach leads to a polynomial of degree 40, resulting in 40 distinct solutions [1-2]. However, the challenging problem is not to find all the solutions, but to directly determine a unique solution among all possible solutions. Two approaches achieve this requirement, namely the iterative approach and the use of additional sensors [3-5]. These approaches have their own disadvantages in terms of complexity and cost. The Jacobian matrix of the system [6] is also of importance in static analysis and velocity kinematics, which in turn required in trajectory control tasks.

In practice, the functionality of linkage would be drastically affected by treating the closed-loop assembly as a compliant mechanism. Monolithic skeleton joining all the links with narrow cross sectional segments forms such compliant mechanism. There are several advantages of these compliant mechanisms and many studies [7-8] revealed the analysis of such compliant parallel linkages. The workspace characteristics, including total (or reachable) and primary (or dexterous) spaces and the singularity characteristics are also important factors in design as well as control coordination of parallel manipulators. The total workspace is the region over which the end-effector can reach with at least one orientation, whereas the primary workspace is that the end-effector can reach with all orientations [9]. Many researchers have addressed the workspace analysis of parallel manipulators and the predominant approach used as seen in the literature in general, has been a geometric mapping. For example, the boundary of the dexterous workspace for a 3-degree of freedom (DOF) planar parallel manipulator was determined by using screw theory [10] and geometric reasoning [11-12]. For a broader class of parallel manipulators, a study to classify the various shapes of workspace due to changes in link lengths was reported in [13] and a formulation of an architecture-independent method based on kinematic mapping can be found in [14]. The manipulator sometimes looses degrees of freedom at some inverse kinematic singularities within the workspace. It is shown that at these instants stiffness of manipulator reaches a maximum value. Several recent works focused on such studies to improve the effectiveness of the manipulation.

In this line, the present work deals with forward and inverse kinematics, workspace and stiffness analysis of parallel manipulators. The forward kinematics solutions are obtained numerically by minimizing the squared-error defined in terms of Cartesian pose vector and the solutions are validated with radial-basis function neural network outputs. Jacobian matrix at a particular platform pose is then obtained and platform stiffness matrix is determined. For the analysis of the link-flexibility and joint compliance effects, a finite element model is proposed with frame and plate elements

along with equivalent torsional stiffness at the joints. This facilitates in evaluation of changes in platform stiffness matrix of manipulator. The stiffness indices are validated with commercial finite element code. The paper is organized as follows: Section-2 deals with the mathematical modelling of illustrated 3-RRR planar parallel manipulator and various indices to represent the kinematic characteristics along with an introduction to the proposed FE model. Section-3 describes the results and discussion.

II.   Mathematical Modelling

The 3-RRR is a three degree-of-freedom planar parallel manipulator. It has a mobile platform and three R-R-R serial chains that join it to a fixed base. Each chain is composed by three rotational revolute (R) joints. As shown in Fig.1, the point P(x,y) is the end-effector position in the global reference frame and ϕ be its orientation. The point O is the origin of the fixed reference frame and the points A_i, B_i, C_i, with i=1,2,3, define the rotational articulations of each limb. Points A_i are actuated, so that the actuators are fixed to the base. Thus, the three fixed pivots A_1, A_2 and A_3 define the geometry of a fixed base and the three moving pivots C_1, C_2 and C_3 define the geometry of a moving platform. Together, the mechanism consists of eight links and nine revolute joints. In the programming of a robot manipulator, typically a set of desired positions and orientation, and perhaps the time derivatives of the positions and orientations of the end-effector are specified in space. The problem is to find all possible sets of actuated joint variables and their corresponding time derivatives which will bring the end-effector to the set of desired positions and orientations with the desired motion characteristics. This process is known as inverse kinematics. On the other hand, sometimes the actuated joint variables and possibly their time derivatives are obtained from reading of sensors installed at the joints, from which all possible sets of end-effector positions and orientations and their corresponding time derivatives are obtained. This procedure is called direct or forward kinematics. The closure loop equations are extremely important in order to analyze and solve these kinematics problems of parallel robots, as they implicitly include the constraints of the mechanism. For direct kinematics of a 3-RRR manipulator, Gosselin [15] showed that a maximum of six solutions are possible. However, due to the trajectory tracking procedure, only one of the solutions is deemed to be correct. Kinematics problems can be solved by various methods such as geometric vector analysis, matrix algebra, direct search and screw-theory.

2.1 Inverse Kinematics
Inverse kinematics of 3-RRR is a straight-forward problem, which is an essential step for the velocity kinematics [16-17]. The base coordinate frame $O-X_0-Y_0$ shown in Fig. 1 is fixed at joint A_1 and a moving or mobile coordinate frame P-X-Y is attached at the center of the moving platform. Let a and h denote the width of the base and moving platforms respectively. It is also assumed that the length of each link in the limb as l.
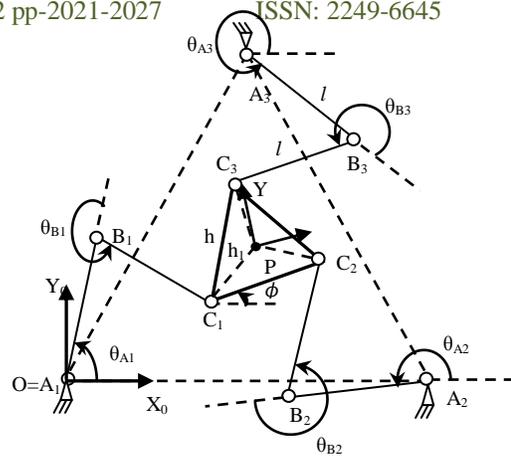
Fig.1 Schematic of 3-RRR Planar Parallel Manipulator

The position vector of point B_i (i=1,2,3) in the base coordinate frame can be expressed as

$$r_{Bi} = r_{Ai} + l\begin{bmatrix} \cos\theta_{Ai} \\ \sin\theta_{Ai} \end{bmatrix}, \qquad i = 1,2,3. \qquad (1)$$

where r_{Ai} and r_{Bi} are the position vectors of joint points A_i and B_i. Also, θ_{Ai} are rotation angles of links A_iB_i. The position vector of C_i can be written as

$$r_{Ci} = r_p + [R]r_{Ci}^p \qquad (2)$$

Here again, r_p is the position vector of P with respect to base coordinate frame $O-X_0-Y_0$ and r^p_{ci} is the position vector of C_i in the mobile frame P-X-Y, $[R] = \begin{bmatrix} \cos\phi & -\sin\phi \\ \sin\phi & \cos\phi \end{bmatrix}$ is the rotation matrix for transforming the coordinate system P-X-Y to $O-X_0-Y_0$ and θ_{Bi} is the rotation angle of links B_iC_i. The constraint equation associated with the ith kinematic chain can be expressed as a second-order norm given by:

$$\|r_{Ci} - r_{Bi}\| = l, \text{ i=1, 2, 3} \qquad (3)$$

These are three equations in-terms of actuation degree of freedom θ_{Ai} for given set of coordinates of P and they correspond to workspace space circles. The above equation (3) can be written as

$$e_{1i} \sin\theta_{Ai} + e_{2i} \cos\theta_{Ai} + e_{3i} = 0 \qquad (4)$$

Based on equation above equation, the inverse kinematics solution for 3-RRR mechanism can be expressed as

$$\theta_{Ai} = 2\tan^{-1}\frac{-e_{1i} \pm \sqrt{e_{1i}^2 + e_{2i}^2 - e_{3i}^2}}{e_{3i} - e_{2i}}, \text{i} = 1,2,3. \qquad (5)$$

where

$$e_{11} = -2l\left(y - \frac{h\sin\phi}{2} - \frac{\sqrt{3}h\cos\phi}{6}\right) \qquad (6)$$

$$e_{21} = -2l\left(x - \frac{h\cos\phi}{2} + \frac{\sqrt{3}h\sin\phi}{6}\right) \qquad (7)$$

$$e_{31} = \left(x - \frac{h\cos\phi}{2} + \frac{\sqrt{3}h\sin\phi}{6}\right)^2 + \left(y - \frac{h\sin\phi}{2} - \frac{\sqrt{3}h\cos\phi}{6}\right)^2 \qquad (8)$$

$$e_{12} = -2l\left(y + \frac{h\sin\phi}{2} - \frac{\sqrt{3}h\cos\phi}{6}\right) \qquad (9)$$

$$e_{22} = -2l\left(x + \frac{h\cos\phi}{2} + \frac{\sqrt{3}h\sin\phi}{6} - a\right) \qquad (10)$$

$$e_{32} = \left(x + \frac{h\cos\phi}{2} + \frac{\sqrt{3}h\sin\phi}{6} - a\right)^2 +$$
$$\left(y + \frac{h\sin\phi}{2} - \frac{\sqrt{3}h\cos\phi}{6}\right)^2 \qquad (11)$$

$$e_{13} = -2l\left(y + \frac{\sqrt{3}h\cos\phi}{3} - \frac{\sqrt{3}}{2}a\right) \qquad (12)$$

$$e_{23} = -2l\left(x - \frac{\sqrt{3}h\sin\phi}{3} - \frac{1}{2}a\right) \qquad (13)$$

$$e_{33} = \left(x - \frac{\sqrt{3}h\sin\phi}{3} - \frac{1}{2}a\right)^2 + \left(y + \frac{\sqrt{3}h\cos\phi}{3} - \frac{\sqrt{3}}{2}a\right)^2 \qquad (14)$$

Taking the time derivative of the Eq. (3) leads to:

$$\begin{bmatrix} D_{11} & 0 & 0 \\ 0 & D_{22} & 0 \\ 0 & 0 & D_{33} \end{bmatrix} \begin{Bmatrix} \dot{\theta}_{A1} \\ \dot{\theta}_{A2} \\ \dot{\theta}_{A3} \end{Bmatrix} = \begin{bmatrix} Q_{11} & Q_{12} & Q_{13} \\ Q_{21} & Q_{22} & Q_{23} \\ Q_{31} & Q_{32} & Q_{33} \end{bmatrix} \begin{Bmatrix} \dot{X} \\ \dot{Y} \\ \dot{\phi} \end{Bmatrix}$$

$$(15)$$

Where

$$Q_{i1} = 2l\cos\theta_{Ai} + e_{2i}/l \qquad (16)$$

$$Q_{i2} = 2l\sin\theta_{Ai} + e_{1i}/l \qquad (17)$$

$$D_{ii} = e_{1i}\cos\theta_{Ai} - e_{2i}\sin\theta_{Ai} \qquad (18)$$

$$Q_{13} = \left(\frac{h\sin\phi}{2} + \frac{\sqrt{3}h\cos\phi}{6}\right)Q_{11} - \left(\frac{h\cos\phi}{2} - \frac{\sqrt{3}h\sin\phi}{6}\right)Q_{12}$$
$$(19)$$

$$Q_{23} = \left(\frac{h\cos\phi}{2} + \frac{\sqrt{3}h\sin\phi}{6}\right)Q_{22} + \left(-\frac{h\sin\phi}{2} + \frac{\sqrt{3}h\cos\phi}{6}\right)Q_{21} \qquad (20)$$

$$Q_{33} = -\frac{\sqrt{3}h\sin\phi}{3}Q_{32} - \frac{\sqrt{3}h\cos\phi}{3}Q_{31} \qquad (21)$$

Equation (15) can be written as: $[J_q]\{\dot{q}\} = [J_X]\{\dot{X}\}$ with $[J_q]$ and $[J_X]$ as two Jacobian matrices; one giving the condition for direct singularity problem and other gives that of the inverse singularity states.

2.2 Forward Kinematics Solutions
       The investigation of forward kinematics issue is important and practical for the manipulation and control of the pose of the parallel manipulator. In present paper, two soft computing tools are proposed based on (i) minimization of positional error of platform joints and (ii) integrating a neural network with inverse kinematics model. Referring to Fig.2, if the six input angles and all the link-lengths are specified, the positions of points C_i are calculated from the following equation [18]:

$$C_i = [A_i + l\cos(\theta_{Ai}) + l\cos(\theta_{Ai} + \theta_{Bi}),$$

$$l\sin(\theta_{Ai}) + l\sin(\theta_{Ai} + \theta_{Bi})], \qquad i = 1, 2, 3$$
$$(22)$$
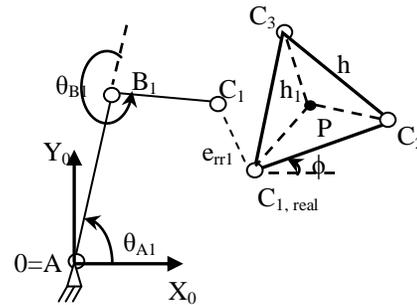
Fig.2 Connectivity of point C_1 in one limb

On the other hand, the real coordinates $C_{i, real}$, are obtained from a set of Cartesian pose vector (x, y and ϕ) of the table centre according to the following inverse relations:

$$C_{1,real} = [\, x - h_1\cos\left(\tfrac{\pi}{6} + \phi\right)\, ,\; y - h_1\sin(\tfrac{\pi}{6} + \phi)]$$
$$(23)$$

$$C_{2,real} = [\, x + h_1\cos\left(\tfrac{\pi}{6} - \phi\right)\, ,\, y - h_1\sin(\tfrac{\pi}{6} - \phi)]$$
$$(24)$$

$$C_{3,real} = [\, x - h_1\sin(\phi)\, ,\, y + h_1\cos(\phi)]$$
$$(25)$$

The connectivity error $f = \sum_{i=1}^{3} e_{rri} = \sum_{i=1}^{3} \|C_{i,real} - C_i\|$, between the two sets of points $C_{i,real}$ and C_i constitutes the objective function to be minimized. When this error is close to zero, the manipulator achieves a desired position and orientation of the mobile platform. In present work, binary coded genetic algorithms (GA) approach is used to obtain the optimum solution. GA [19-20] is computational method meant to solve complex and nonlinear optimization problems. They are inspired by the genetic processes of living organisms. In nature, individuals of a population compete for basic resources. Those individuals achieving better surviving rates have higher probabilities to attract possible partners and to generate descendants. As a consequence, best adapted individuals' have higher chances to be passed on to the next generations. GA, in order to emulate this behavior, works with a population of individuals. Each individual represents the possible solution of a problem (for example the best set of features to identify disruptions). The quality of each individual in evolutionary terms is evaluated on the basis of a fitness function. A higher probability to have descendants is assigned to those individuals with better fitness functions. The most promising areas of the searching space are explored by favoring the crossing between the better adapted individuals.

       Neural networks are noted for the ability of complex functions learning and relationship building, which led to their extensive applications including pattern classification, function approximation and optimization. They can be utilized to address the forward kinematics problem of parallel manipulators. As the solution of inverse kinematics problem for parallel manipulators is simpler than forward kinematics problem, neural network addresses the forward kinematics model through the use of inverse kinematics solution. Training set for neural network is selected out of the set of

inverse kinematics solutions. Discrete points of each actuated joint are taken as inputs and corresponding poses about the motion of platform center are considered as outputs. The neural network is trained using the above off-line training set and gives the solution of the forward kinematics model. In present work, conventional radial basis function network [21] with a nonlinear hidden layer and a linear output layer is employed. Each of the units in hidden layer applies a fixed-feature detector which uses a specified kernel function (Gaussian) to detect and respond to localized portions of the input vector space. The network output is a weighted linear summation of the output of the hidden neurons. This network is a universal function approximates that demonstrates more robustness and flexibility than traditional regression approaches such as polynomial fits. Fig.3 shows the proposed methodology of solving forward kinematics.

2.3 Workspace of the linkage

An important characteristic of a parallel manipulator is its workspace. Several types of workspaces have been proposed, such as the constant orientation workspace, the maximal workspace, the inclusive maximal workspace, and the dexterous workspace. The constant orientation workspace of a planar parallel mechanism can be found as the intersection of annular regions corresponding to the reachable workspaces of its kinematics chains.
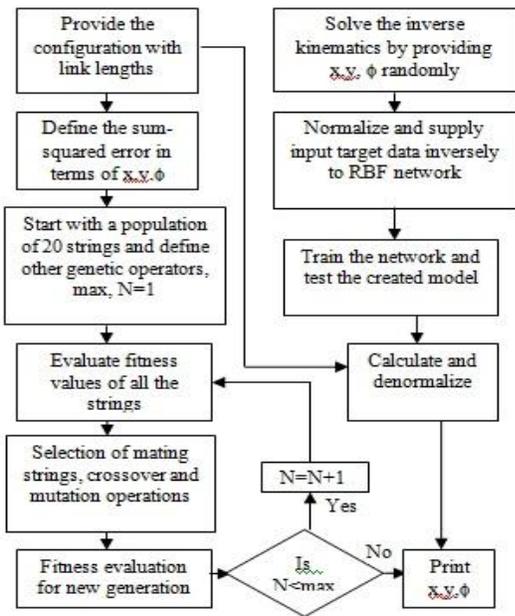
Fig.3 Flowchart for the forward kinematics methodology

The equations of workspace circles can be expressed as [16]:

$$(x+C_{ix}'\cos\phi - C_{iy}'\sin\phi -A_{ix})^2 + (y + C_{ix}'\sin\phi + C_{iy}'\cos\phi -A_{iy})^2 =(l_1 \pm l_2)^2 \qquad (26)$$

Here l_1 and l_2 are the lengths of links A_iB_i and B_iC_i respectively. The prime ' indicates that coordinate measurement is with respect to mobile frame of reference. Thus, workspace essentially depends on x,y and ϕ. If $l_1 \neq l_2$,

there are two concentric circles correspond to every center. In practice, the link lengths are taken identical in most of the cases.

2.4 Jacobian analysis

Let the actuated joint variables and the location of the moving platform be denoted by the vectors q and x, respectively. Then the kinematic relations can be written in the general form as f(x,q)=0 where f is the function of x=(x, y, ϕ)^T and q=(θ_{A1}, θ_{A2}, θ_{A3})^T and 0 is an n-dimensional zero vector. The variables x, y and Φ are the coordinates of the end-effector point P with respect to the base and orientation of the platform, respectively. Moreover, θ_{A1}, θ_{A2} and θ_{A3} denote actuated joints. Differentiating the f with respect to the time, $[J_X]\{\dot{X}\} + [J_q]\{\dot{q}\}=0$ is obtained. Here $\dot{x}$ and $\dot{q}$ are the time derivatives of x and q, respectively. Here $[J_q]$ and $[J_X]$ are two separate Jacobian matrices. The overall Jacobian matrix for a parallel manipulator can be obtained as $[J] = [J_q]^{-1}[J_X]$ and also corresponding stiffness

2.5 Stiffness Analysis & Dexterity index

The value of stiffness evolves according to the geometry, topology of the structure and position and orientation of the platform within the workspace. The stiffness of a parallel robot at a given point of its workspace can be characterized by its stiffness matrix. This matrix combines the forces and moments applied to the platform. For rigid body model, the stiffness matrix is defined as follows [22]:

$$[S]=k[J]^{-T}[J]^{-1} =k([J][J]^T)^{-1} \qquad (27)$$

where k is the stiffness of actuated joint which is assumed to be same for all the joints. The condition number is quite often used as an index to describe the accuracy/dexterity of a robot and the closeness of a pose to a singularity. Condition number of a matrix is used in numerical analysis to estimate the error generated in the solution of a linear system of equations by the error on the data. When applied to the Jacobian matrix, the condition number will give a measure of the accuracy of the Cartesian velocity of the end-effector and the static load acting on the end-effector. The dexterity of a manipulator can be denoted as the condition number of its Jacobian matrix. Dexterity has recently emerged has a measure for manipulator kinematic performance.

2.6 Finite element model

Links are considered as flexible members undergoing flexural and axial deformations. For analysis of flexibility effects, each limb (i=1,2,3) of the manipulator is discretized with frame elements and therefore the stiffness matrix for each of the three limbs is calculated as an assemblage of individual link stiffness matrices. In present case, there are three degrees of freedom at each node namely axial deformation (u) and bending deflection (v) and slope (θ) as shown in Fig.4.
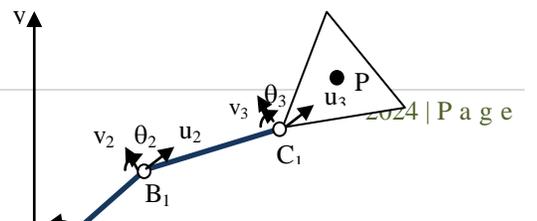
(mm)	0	0	0	900	450	779
Mobile joints (mm)	C_1		C_2		C_3	
	x	y	x	y	x	y
	414	230	493	244	441	305

Fig.4 Finite element model

The unknown displacements at the joints are calculated from the applied joint torques and the elemental forces and corresponding stresses are obtained. Joint compliance is considered as a torsional spring in our pseudo-rigid body model. Here the joint is approximated as a narrow rectangular cross-sectioned element, whose spring constant is given as [23] $(E_n I_n)/l_n$, where E_n is the elastic modulus, I_n is the moment of inertia of narrow cross-section which is equal to $\frac{1}{12}bt^3$, for rectangle. Here, b,t,l_n are respectively width, thickness and length of the section.

III.   Results and Discussion

The parameters of the manipulator considered in the present analysis are depicted in Table-1. The material chosen is steel with density $\rho=7800kg/m^3$ and elastic modulus E= $2.1\times10^5 N/mm^2$. This data is needed during the finite element modelling.

Table-1.Dimensional Parameters of Manipulator[24]:

Parameter	Dimension (mm)
Length of each link	400
Thickness of each link	6
Width of each link	23
Side length of the moving platform	80
Side length of the fixed platform	900
Thickness of the moving & fixed platform	25
Length of the narrow cross-section	40
Thickness of the narrow cross-section	1.5
Width of the narrow cross-section	23

Table-2 shows the input configuration of the manipulator in terms of the base and mobile platform coordinates.

Table-2.The 3-RRR planar parallel manipulator configuration

Base Joints	A_1		A_2		A_3	
	x	y	x	y	x	y

First, the genetic algorithm with uniform crossover and mutation used in finding forward kinematic solution has a crossover rate of 0.999 and mutation rate of 0.001. The high crossover rate ensures that maximum global search. The population size is taken as 40, and the outputs are tested by varying the number of generations. The variable ranges considered in the present task are shown in Table-3.

Table-3.The upper and lower bounds of the design variables.

Design variables	Variable limits
Cartesian coordinate moving platform (x)	[0 – 600 mm]
Cartesian coordinate moving platform (y)	[0 – 600 mm]
Angle of the moving platform (ϕ)	$[-360^0 - 360^0]$

During neural network analysis, initially an inverse kinematics problem is solved by geometric method for a range of Cartesian coordinates of the end-effector X, Y and φ chosen according to X=[445,450 mm], Y=[255,262 mm] and φ=[-10° 10°]. Now RBF neural network model is trained with the output of the above inverse kinematics solution as input data, while the corresponding Cartesian coordinates are treated as target data. The number of training patterns taken here are 1008 and the spread constant employed is 1.0. Table-4 shows the comparison forward kinematic solution with genetic algorithms and neural networks.

Table-4. Forward kinematic solution using Genetic Algorithms and Neural networks

Method	No.of Iterations	X (mm)	Y (mm)	φ (deg)
GA	5000	449.85	260.41	9.50
	6000	451.61	259.82	9.50
Neural networks	1008	448.94	257.64	10.18
	1008	451.81	259.34	9.78

It is observed that the results obtained from genetic algorithms and neural networks are very close to each other. Fig.5 shows the fitness variation with number of iterations in genetic algorithms.
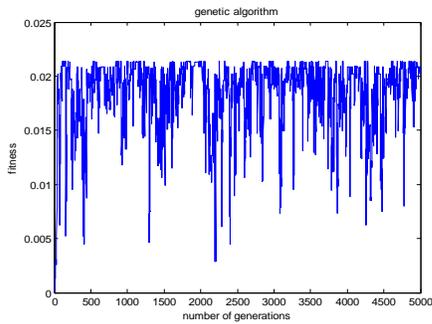
Fig.5 Fitness Vs number of generations

The performance curve for neural network is shown in Fig.6.
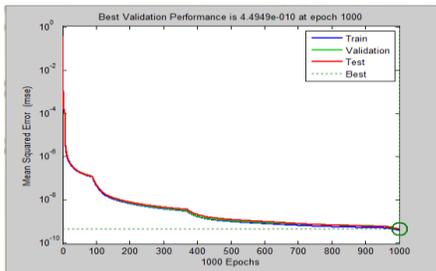
Fig.6 Graph of Training Performance in neural network

The constant orientated workspace is plotted for different angles of the moving platform as shown in Fig.7 and it is observed that the area of the workspace decreases when ϕ varies from 0° to 30°. The dexterity of a mechanism can be considered as its ability to perform small displacements of its end effector at a specified pose of its workspace. It is based on the condition number of the homogeneous Jacobian matrix here the inverse condition number is mapped on a constant orientation workspace to determine the dexterity of the manipulator as shown in Fig.8. It is well known that as inverse condition number is equal to 1 represents a perfect isotropic dexterity and 0 represents singular configuration. Here in Fig.8 all the values around the boundary of the workspace are close to zero, indicating the singularity regions. In order to verify and examine the static performance, a finite element model is prepared. The analysis is carried out using the ANSYS (V13) software.

(a) $\phi=0^o$

(b) $\phi=30^o$
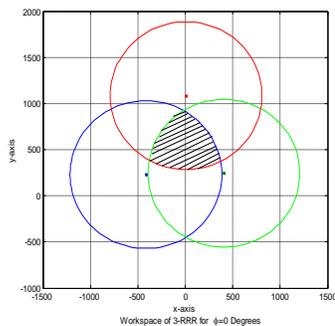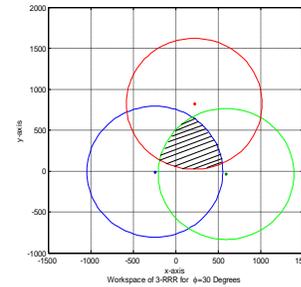
Fig.7 Constant orientation work spaces at X=450mm, and Y=259.81mm
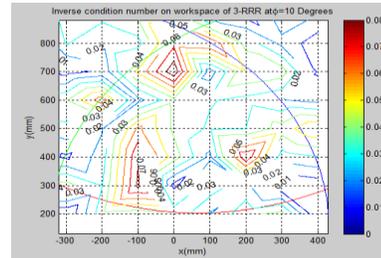
Fig.8 Inverse condition number mapping on constant orientation workspace

The distributions for the scaled minimum stiffness are illustrated in Fig.9. It can be observed that, the distribution of stiffness in a x–y plane the lowest value of minimum stiffness occurs around the boundary of the workspace, where the manipulator approaches direct singularities.
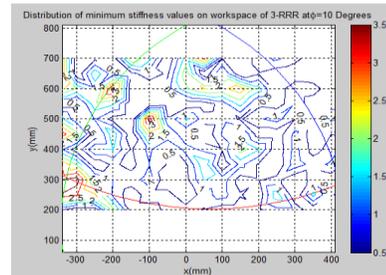
Fig.9 Distribution of minimum stiffness on constant orientation workspace

The finite element model is built based on the original geometrical prototype dimensions, as shown in Fig.10,
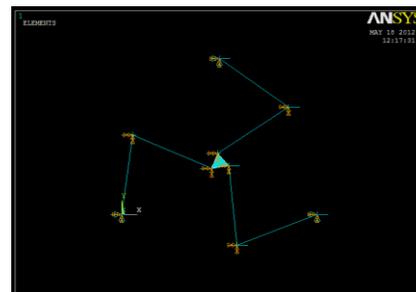
Fig.10 ANSYS image of the model

2-D BEAM188 elements with realistic parameters for limbs and four-node SHELL181 element for moving platform and at each joint combination14 (spring constant) are

adopted to mesh the model. Forces are applied on the actuated joints so as to get a deformation on the moving platform. The displacements of the model at each node are carefully examined. The analysis results are close to the theoretical outputs as shown in Table-5.

Table-5.Displacement of the end-effector at each node

S.No	Displacements at the end-effector (mm)	
	Theoretical	ANSYS
1	0.0010	0.0022
2	0.0014	0.0023
3	0.0000	0.0021

And also the stiffness at one platform pose (i.e., x=450mm, y=259.81mm, $\phi=10^o$) of the moving platform is presented. Here, it is observed that the trace of the Jacobian matrix of the rigid body model as -0.123. The manipulator stiffness is estimated from the nodal displacements and corresponding reaction forces in the finite element model. Using ANSYS software, it is found to be 0.1007×10^9 N/mm, which is quite larger than 0.816×10^5 N/mm as obtained from conventional rigid body model with Jacobian matrix. The discrepancy of stiffness may be due to mismatch of the degrees of freedom in the elements under consideration for meshing.

IV. Conclusions

This paper has presented forward kinematic solutions for rigid body model using genetic algorithms and neural networks and also a constant orientation workspace is calculated. Within this workspace, Jacobian and stiffness analysis are conducted and to know the performance of the manipulator the inverse condition number and minimum stiffness values are plotted. Finally at one particular platform pose, finite element model is developed in ANSYS and displacements of the end-effector and stiffness index values are estimated.

REFERENCES

[1]   M. L. Husty, An algorithm for solving the direct kinematics of general Stewart-Gough platforms, *Journal of Mech. Mach. Theory, 31(4),*1996, 365-380.

[2]   M. Raghavan, The Stewart platform of general geometry has 40 configurations, *ASME Journal of Mech. Design, 115,* 1993, 277-282.

[3]   Y. Wang, A direct numerical solution to forward kinematics of general Stewart-Gough platforms, *Journal of Robotica, 25(1)*, 2007, 121-128.

[4]   J-P. Merlet, Closed-form resolution of the direct kinematics of parallel manipulators using extra sensors, *Proc. IEEE Int. Con. Robotics and Automation,* 1993, 200-204.

[5]   I. A. Bonev, J. Ryu, S-G. Kim and S-K. Lee, A closed-form solution to the direct kinematics of nearly general parallel manipulators with optimally located three linear extra sensors, *IEEE Trans. Robot. And Automation, 17(2),* 2001, 148-156.

[6]   Gosselin C, Dexterity Indices for Planar and Spatial Robotic Manipulators, *IEEE International Conference on Robotics and Automation, Cincinnati, OH, USA,* 1990, 650-655.

[7]   Alba, O. G., Pamanes, J. A. Wenger, P., Trajectory planning of a redundant parallel manipulator changing of working mode, *proc.12th IFToMM World Congress.* 2007, 18-21.

[8]   A. Ghafoor, J.S. Dai and J. Duffy, Stiffness Modelling of the Soft Finger Grasp in Robotic Applications, *Submitted to ASME Journal of Mechanical Design*, 2001.

[9]   M. Griffis and J. Duffy, Global stiffness modelling of a class of simple compliant coupling, *Journal of Mech. Mach. Theory, 28(2),* 1993, 207-224.

[10]   Ming Z. Huang, Jean-Lue Thebert, A study of workspace and singularity characteristics for design of 3-DOF planar parallel robots", *Int.J.Adv Mannuf Technol., 51,* 2010, 789-797.

[11]   Pennock GR, Kassner DJ, The workspace of a general geometry planar three-degree-of-freedom platform-type manipulator, *ASME Journal of Mech. Design 115,* 1993, 269–276.

[12]   Merlet J-P, Gosselin C, Mouly N, Workspace of planar parallel manipulators, *Journal of Mech. Mach. Theory, 33*, 1998, 7–20.

[13]   Gao F, Liu X-J, Chen X, The relationships between the shapes of the workspaces and the link lengths of 3-DOF symmetrical planar parallel manipulators, *Journal of Mech. Mach. Theory, Mech. Mach. Theory, 36,* 2001, 205–220.

[14]   Hayes MJD, Architecture independent workspace analysis of planar three-legged manipulators, *In: Proceedings of the workshop on fundamental issues and future research directions for parallel mechanisms and manipulators*, Quebec City, Quebec, Canada, 2002.

[15]   C. Gosselin, J. Angeles, *Kinematics of Parallel Manipulators*, PhD Thesis, McGill University Montreal, Quebec, Canada, 1989.

[16]   M.Arsenault and R.Boudreau, The synthesis of three degree of freedom planar parallel mechanism with revolute joints (3-RRR) for an optimal singularity-free workspace, *Journal of Robotic Systems, 21,* 2004, 259-274.

[17]   Jun Wu, Jinsong Wang, Zheng You, A comparison study on the dynamics of planar 3-DOF 4-RRR, 3-RRR and 2-RRR parallel manipulators, *Journal of Robotics and Computer-Integrated Manufacturing, 27,* 2011, 150–156.

[18]   Lucas Weihmann, Daniel Martins ans Leandro dos Santos Coelho, Modified differential evolution approach for optimization of planar manipulators force capabilities, *Journal of Expert systems with Applications, 39,* 2012,6150-6156.

[19]   L. Rolland, Synthesis on the forward kinematics problem algebraic modelling for the planar parallel manipulator, *Journal of Adv. Robotics, 20*, 2006, 1035–1065.

[20]   Rohitash Chandra a, Luc Rolland, On solving the forward kinematics of 3RPR planar parallel manipulator using hybrid metaheuristics, *Journal of Applied Mathematics and Computation, 217,* 2011, 8997–9008.

[21]   Dan Zhang and ZhenGao, Forward kinematics, performance analysis, and multi-objective optimization of a bio-inspired parallel manipulator, *Journal of Robotics and Computer-Integrated Manufacturing, 28,* 2012, 484–492.

[22]   Ridha Kelaiaia, Olivier Company and Abdelouahab Zaatri, Multi objective optimization of a linear Delta parallel robot, *Mechanism and Machine Theory, 50,* 2012, 159–178.

[23]   Engin Tanik, Transmission angle in compliant slider-crank mechanism, *Journal of Mechanism and Machine Theory , 46(11),* 2011, 1623–1632.

[24]   Yue-Qing Yu, Zhao-Cai Du, Jian-Xin Yang, and Yuan Li, An Experimental Study on the Dynamics of a 3-RRR Flexible Parallel Robot, *IEEE Transactions on Robotics, 27(5),* 2011, 992-997.